COMPARISON OF EXPERIMENTAL, SEMI-EMPIRICAL AND NON-LINEAR FINITE ELEMENT ANALYSES OF NUCLEAR CONTAINMENT STRUCTURES FOR IMPACT LOADS

R.M. Parmar, T. Singh, R.K. Singh, K.K. Vaze
Reactor Safety Division, Bhabha Atomic Research Centre, Trombay, Mumbai, INDIA-400085
E-mail of corresponding author: rparmar@barc.gov.in

ABSTRACT

Containment structures are designed not only to provide leak tight barrier against release of radioactivity but also play a role in ensuring that it can withstand the impact load from projectile or missile impacts or internal plant accidents. In assessing the containment structures of nuclear power plants, predicting the characteristics of impact resistance in relation to design and safety considerations is relevant. The impact may result from missiles, aircraft crash, and internal accidents. Therefore the impact resistance of the concrete should be known, for design and safety of the containment structures. Here an attempt has been made to work out the analysis of the reinforced concrete target due to an impact in terms of penetration, spalling, scabbing and perforation. The experiments done by Sugano et al [1] have been simulated in the present analysis. The results from present finite element analysis are then compared with the experimental results as well as empirical/semi-empirical and analytical solutions. The results of the finite element analysis agree well with the experimental results and describe the failure of different structural members more realistically as compared to the empirical/semi-empirical and analytical solutions. And therefore it is recommended to use finite element analysis rather than empirical/semi-empirical and analytical solutions, to determine the impact resistance of the structure

INTRODUCTION

In this paper an attempt has been made to work out the analysis of the reinforced concrete target upon an impact of aircraft in terms of penetration, spalling, scabbing and perforation. The experiments done by Sugano et al [1] have been taken for the present analysis. The results from present finite element analysis are then compared with the experimental results as well as empirical/semi-empirical and analytical solutions. The results of analysis with the finite element analysis agree well with the experimental results than other empirical/semi-empirical and analytical solutions. And therefore it is recommended to use finite element analysis rather than empirical/semi-empirical and analytical solutions, to determine the impact resistance of the structure in a more realistic manner as compared to these conventional oversimplified methods.

The full scale experimental details are summarized in the Table 1 and Table 2.

Table 1: Test parameters [1]

Test parameter: Scale factor:	Full-Scale Tests 1/1
Missile	
Type	Deformable missile
Weight (kgf)	about 1500
Diameter (mm)	about 760.0
Velocity (m/s)	215
Target	
Width X height (mm)	7000 X 7000
Thickness (mm)	900-1600
Rebar	
Bending rebar (p_o)	0.4%
Shear rebar	Not provided
Concrete	
Concrete strength(f_c) (MPa)	23.5

Table 2: Detailed test conditions [1]

Missile		Test Panel			
Type of rigidity	Weight (kgf)	Panel	Length (mm)	Width (mm)	Thick. (mm)
GE-J79 Engine	1764	L1	7000	7000	900
GE-J79 Engine	1734	L2	7000	7000	1150
GE-J79 Engine	1781	L3	7000	7000	1350
GE-J79 Engine	1767	L4	7000	7000	1600

EVALUATION OF IMPACT FORCE TIME HISTORY

The impact time history calculated by Sugano et al [1] based on method by K. Muto et al [1] has been used in the analysis. The impact time history has been calculated which is based on the mass distribution of the actual GE-J79 engine and acceleration records from on-board accelerometers and still prints of high speed photographs used for measuring missile's deceleration. Based on this velocity reduction curve and the mass distribution curve, an impact force-time function is derived.

MATERIAL PROPERTIES

The stress strain curve of the concrete is modeled as a tri-linear curve and that of the steel reinforcement is modeled as a bilinear relationship as shown in Fig. 1 and Fig. 2. The concrete damaged plasticity model has been used for modeling concrete.

Concrete properties:

Young's modulus, E	25770 MPa
Poisson's ratio, ν	0.18
Density, ρ	2500 kg/m^3
Dilation angle, ψ	36^0
Compressive initial yield stress, σ_{co}	15.06 MPa
Compressive ultimate stress, σ_{cu}	30.40 MPa
Plastic strain at failure, ε_f	0.35%
Tensile failure stress, σ_{to}	2 MPa
σ_{bo}/σ_{co}	1.16
K	0.67

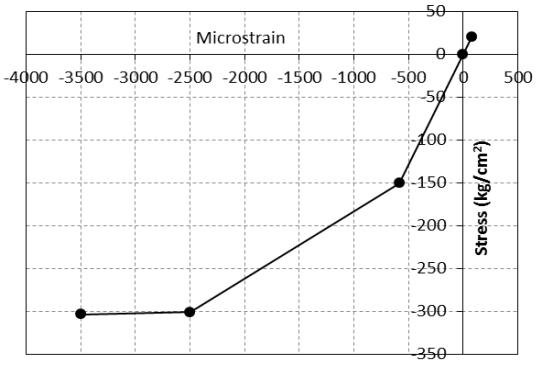

Fig. 1: Stress strain relationship for concrete [1]

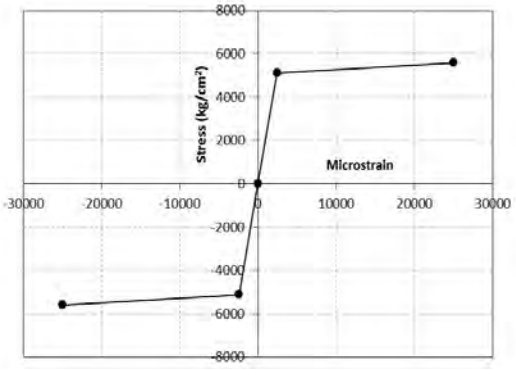

Fig. 2: Stress strain relationship for steel [1]

CONCRETE MATERIAL MODEL

For the present work Concrete damaged plasticity model has been used for the numerical simulation. The main ingredients of the in viscid concrete damaged plasticity model are as follows.

A. Strain rate decomposition

Additive strain rate decomposition is assumed for the rate-independent model:

$\dot{\varepsilon} = \dot{\varepsilon}^{el} + \dot{\varepsilon}^{pl}$ where $\dot{\varepsilon}$ is the total strain rate, $\dot{\varepsilon}^{el}$ is the elastic part of the strain rate, and $\dot{\varepsilon}^{pl}$ is the plastic part of the strain rate.

B. Stress-strain relations

The stress-strain relations are governed by scalar damaged elasticity:

$\sigma = (1-d)D_0^{el} : (\varepsilon - \varepsilon^{pl}) = D^{el} : (\varepsilon - \varepsilon^{el})$

Where

D_0^{el} = initial (undamaged) elastic stiffness of the material;

$D^{el} = (1-d)D_0^{el}$ = Degraded elastic stiffness; and

d = Scalar stiffness degradation variable, which can take values in the range from zero (undamaged material) to one (fully damaged material).

Damage associated with the failure mechanisms of the concrete (cracking and crushing) therefore results in a reduction in the elastic stiffness. Within the context of the scalar-damage theory, the stiffness degradation is isotropic and characterized by a single degradation variable, *d*.

Following the usual notions of continuum damage mechanics, the effective stress is defined as

$$\bar{\sigma} = D_0^{el} : (\varepsilon - \varepsilon^{pl})$$

The Cauchy stress is related to the effective stress through the scalar degradation relation:

$$\sigma = (1-d)\bar{\sigma}$$

The evolution of the degradation variable is governed by a set of hardening variables, $\tilde{\varepsilon}^{pl}$ and the effective stress; that is, $d = d(\bar{\sigma}, \tilde{\varepsilon}^{pl})$

FINITE ELEMENT MODEL

The concrete damaged plasticity model has been used for modeling concrete for the present analysis. The concrete has been modeled using eight node linear brick elements with reduced integration. The rebar have been modeled with 2-node three dimensional truss elements. The reinforcements were embedded in the concrete using the embedded elements.

The mesh has been refined in the impact zone. The mesh density was reduced as the distance from the impact area increases. Sufficient number of elements was taken in the thickness direction. The minimum size of element was taken as 60mm considering maximum size of aggregate in concrete as 25mm. Care was also taken to maintain correct aspect ratio in the grid especially in and around the impact zone. The aspect ratio was increased towards the periphery of the target panel. The time-history loading was then applied over a circular area of radius 400mm at the center of target. The time history loading, as shown in Fig. 3 has been applied at the center of the panel over a circular area of 400mm. Dynamic explicit method has been used for the analysis. The analysis was performed for 80ms.

The finite elements mesh details are summarized in Table 3.

Table 3: Finite Element Mesh Details

Panel	Total Number of elements	Number of elements along thickness
Panel L1	65544	12
Panel L2	35451	9
Panel L3	54610	10
Panel L4	49994	14

The finite element model of the target panel prior to the application of load for panel L1, L2, L3 and L4 are as shown in the Fig. 4, Fig. 5, Fig. 5 and Fig. 6 respectively. Typical model showing support conditions is as shown in Fig. 7. Typical model showing reinforcements is as shown in layer Fig. 8.

Boundary Conditions: The panel has been supported on four square columns of 400mm, at distance of 750mm from the edge of the panel. Since the details of the supporting columns is not known, all the panels have been analyzed springs of stiffness of 10^3 N/m, 10^6 N/m and 10^9 N/m, keeping all the other parameters unchanged. The influences of varying stiffness of the column on the overall panel damage have been studied.

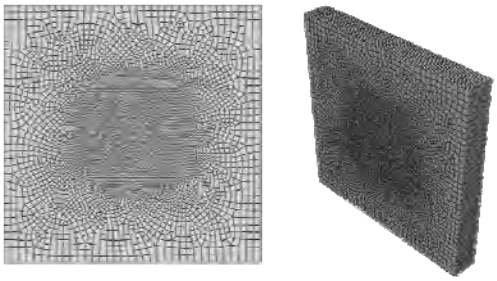

Fig. 3: A typical 3-D finite element model for panel L1 (7mx7m, 900mm thick)

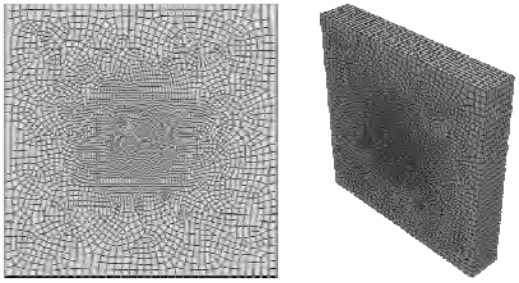

Fig. 4: 3-D Finite element model for panel L2 (7mx7m, 1150mm thick)

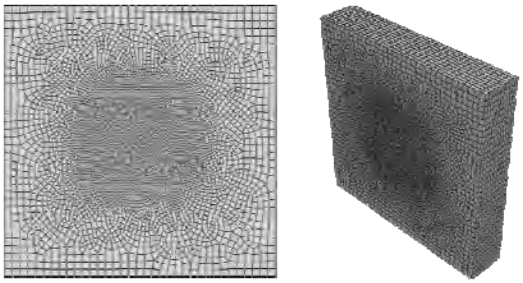

Fig. 5: 3-D Finite element model for panel L3 (7mx7m, 1350mm thick)

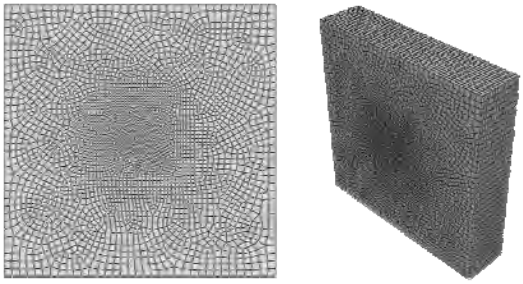

Fig. 6: 3-D Finite element model for panel L4 (7mx7m, 1600mm thick)

Fig. 7: Typical model showing support conditions

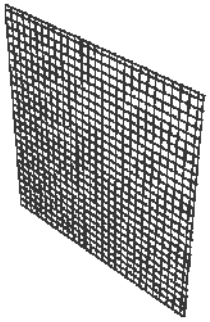

Fig. 8: Typical model showing reinforcement layer

COMPUTATIONAL RESULTS AND DISCUSSION

The observed damage of the test panels is classified into the following five modes;

a) Perforation Mode: The missiles pass through the target completely (marked with a symbol 'P')
b) Just Perforation Mode: The missile does not pass through the target, but is stuck into it, or 'a large opening occurs with many broken rebar but the perforation mode is barely prevented (marked with a symbol 'JP').
c) Scabbing Mode: Considerable concrete debris is peeled off the rear surface of the target, and a small opening appears (marked with a symbol 'S').
d) Just Scabbing Mode: Few small pieces of concrete debris are peeled off the shear cone cracks formed on the rear surface of the target, but the scabbing mode is barely prevented (marked with a symbol 'JS').
e) Penetration Mode: A crater is formed on the front surface of the target, but no scabbing occurs on the rear surface with only radial and shear cone cracks (marked with a symbol 'C').

The results of the finite element model have been summarized in Table 4.

Table 4: Results of Finite Element Model

Panel	V	Experimental results			Numerical Results From FE model		
		Mode	Dimension of crater (mm)		Mode	Dimension of crater (mm)	
			Front depth	width x height		Front depth	width x height
L1	205	JP	Boring	4000 x 7000	JP	Boring	4000 x 7000
L2	215	S	270	3800 x 5400	S	300	3800 x 5400
L3	215	JS	65	Just Scabbing	JS	100	Just Scabbing
L4	215	C	70	Radial Cracks	C	115	Radial Cracks

The results of the finite element model for various panels showing stiffness degradation at the end of the impact are as shown in Fig. 9, Fig. 10, Fig. 11 and Fig. 12.

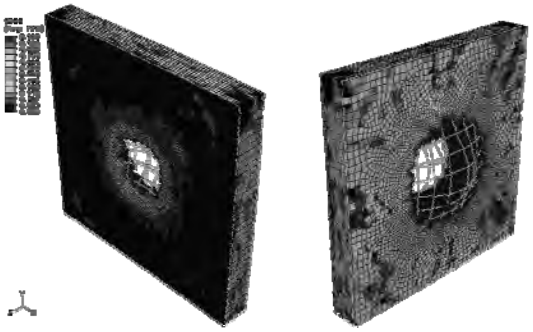

Fig. 9: Three dimensional view of panel L1- Front and back face (Stiffness Degradation)

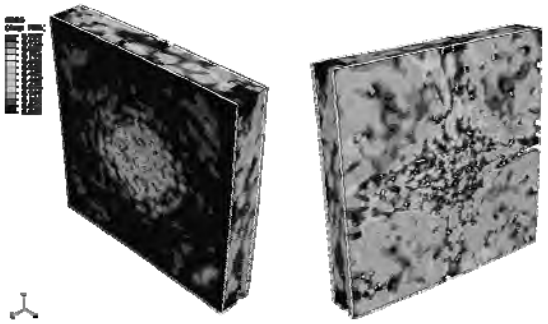

Fig. 10: Three dimensional view of panel L2- Front and back face (Stiffness Degradation)

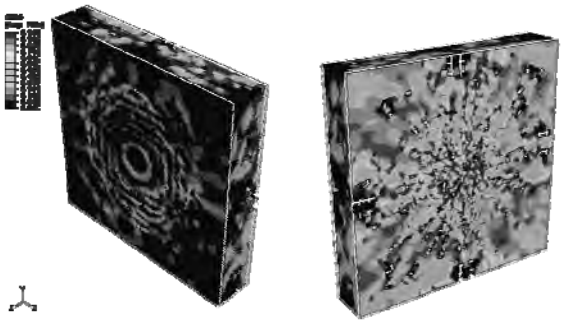

Fig. 11: Three dimensional view of panel L3- Front and back face (Stiffness Degradation)

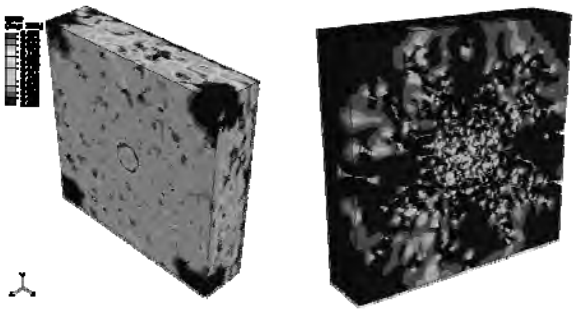

Fig. 12: Three dimensional view of panel L4- Front and back face (Stiffness Degradation)

The energy calculations have been carried out in order to understand the behavior of the panel and to study the energy dissipation during the impact. The energy curves for the whole model for all the panels have been studied and summarized in the Table 5. The energy curves for Panel-L1 are as shown in Fig. 13 to Fig. 20.

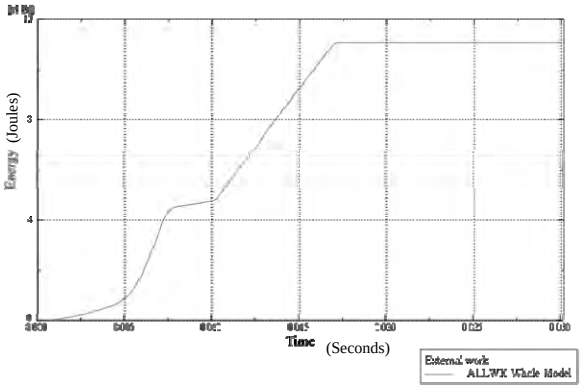

Fig. 13: External work for Panel L1

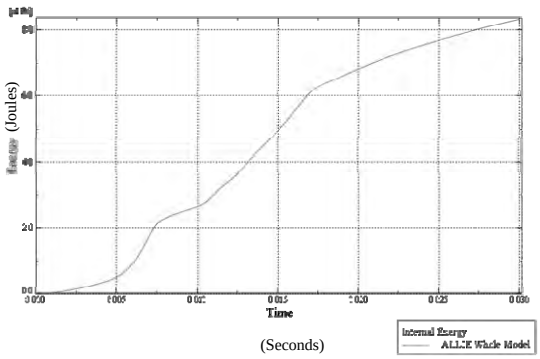

Fig. 14: Internal energy for Panel L1

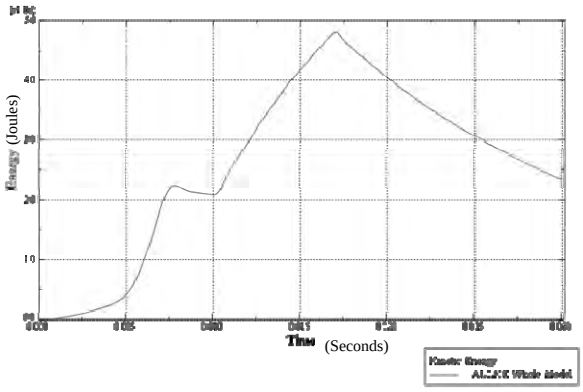

Fig. 15: Kinetic energy for Panel L1

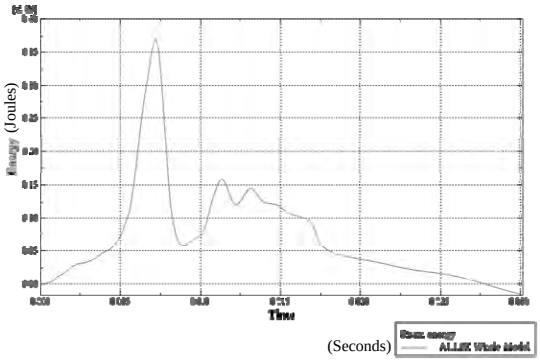

Fig. 16: Strain energy for Panel L1

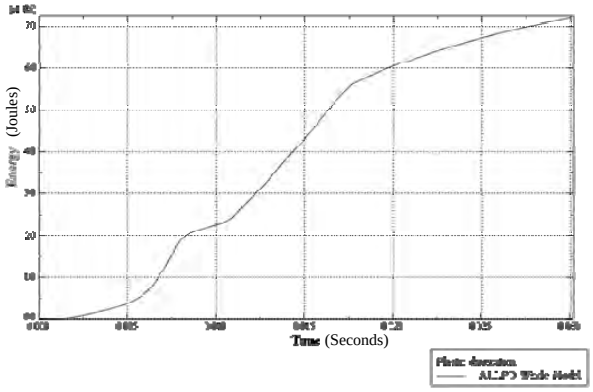

Fig. 17: Plastic dissipation for Panel L1

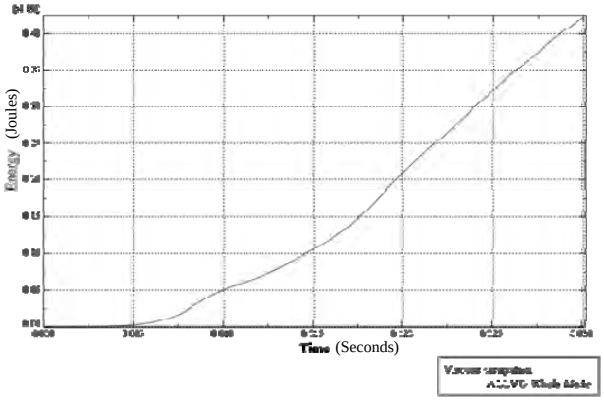

Fig. 18: Viscous dissipation for Panel L1

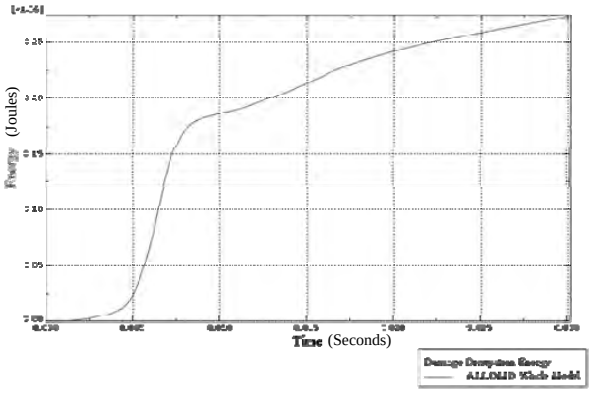

Fig. 19: Damage dissipation energy for Panel L1

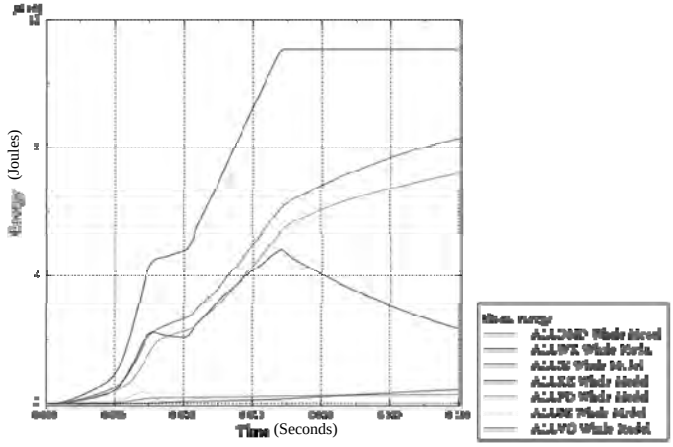

Fig. 20: All energy plot for Panel L1

Table 5: Maximum Energy over the Entire Impulse Duration (Whole Model)

Panel→	Panel-L1	Panel-L2	Panel-L3	Panel-L4
Total work (kJ)	11079.5	3646.1	2385.5	1761.9
Internal Energy (kJ)	8321.1	3038.4	1866.1	1313.1
Kinetic Energy (kJ)	4819.0	1276.9	749.4	499.7
Strain Energy (kJ)	372.2	101.8	125.8	130.8
Viscous dissipation (kJ) (% Dissipation)	422.4 (3.81)	248.7 (6.82)	275.4 (11.54)	248.7 (14.11)
Damage Dissipation Energy (kJ) (% Dissipation)	272.7 (2.46)	212.718 (5.83)	204.5 (8.57)	196.5 (11.16)
Plastic dissipation (kJ) (% Dissipation)	7210.2 (65.08)	3010.6 (82.57)	1905.3 (79.87)	1313.1 (74.53)
Total % dissipation (Viscous + Damage + Plastic dissipation)	71.35%	95.22%	99.98%	99.8%

In addition, the perforation thickness, scabbing thickness and penetration thickness have been calculated using empirical and semi-empirical approaches like NDRC, MNDRC etc. available in the literature and widely used in the industry for the design purposes. The results are summarized in the Table 6.

Table 6: Summary of Results of Empirical/Semi Empirical Formulae

Panel→	Panel-L1	Panel-L2 And Panel- L3	Panel-L4	Remarks
Empirical/Semi empirical formula	Perforation Thickness (mm)	Scabbing Thickness (mm)	Penetration Thickness (mm)	NDRC – National Defense Research Committee MNDRC- Modified National Defense Research Committee MBRLF- Modified Ballistic Research Laboratory formula BRL – Ballistic Research Laboratory
NDRC	1910.7	2686.9	2185.6	
MNDRC	1910.7	2686.9	2185.6	
MBRLF	1957.9	-	663.9	
CKW-BRL	827.4	-	-	
Bechtel	-	2257.8	-	
Haldar	-	707.1	-	

The panel L1 is found to fail in perforation mode, Panel L2 and L3 fail either in scabbing or just scabbing mode and L4 has been observed to fail in penetration mode both in experimental and present finite element analysis. However this is not reflected in the calculation/estimation from the empirical equations. None of the results of Empirical/Semi empirical formulas provide reasonable estimation and are over-conservative and suitable for preliminary design only.

Comments based on studies: In the present analysis, springs have been modeled as the support condition for the concrete panels. Since the stiffness of the backup structure was not known, it has been assumed arbitrarily for all the four panels. The panels L1, L2, L3 and L4 have been run with the assumed stiffness of 10^3 N/m, 10^6 N/m and 10^9 N/m with all the other parameters unchanged. The influences of the spring stiffness on damage to the concrete have been studied in terms of penetration, spalling, scabbing and perforation in the parametric study. And therefore checks on the displacement have not been done and only the damage to the panel has been studied.

Influence of support boundary: The damage is completely localized and the support boundary stiffness has a little influence on the damage, observed in the finite element model as well as during the experiment also.

The penetrations have been observed to be higher than experimental results in all four finite element models. The reason may the confinement of the concrete. The confinement of the concrete has not been modeled in the present analysis. This may be the reason why the numerical results are on higher side than the experimental results. A large energy is utilized during penetration due to confinement of the concrete; this huge energy has not

been captured in the present finite element model, as only unconfined uniaxial properties of the concrete have been used in the model.

CONCLUSION

The impact resistance of the concrete should be known, for design and safety of the structure. Local damage consists of spalling of concrete from the front (impacted) face and scabbing of concrete from the rear face of the target together with missile penetration into the target. If damage is sufficient the missile may perforate or pass through the target. Overall dynamic response of the target wall consists of flexural deformations and a potential flexural or shear failure if the strain energy capacity of the wall does not exceed the kinetic energy input to the wall

The numerical, empirical, and semi-analytical methods for evaluation of penetration, spalling, scabbing and perforation of concrete target by missile or any other impact and the limitations of each method have been studied. The empirical/semi-empirical methods are not accurate as these methods are essentially based on the experimental results; they are valid in the range in which they have been derived. Hence it is recommended to use Finite Element Analysis for prediction of the damage in terms of spalling, scabbing, penetration, perforation etc.

REFERENCES

[1] T. Sugano , H. Tsubota , Y. Kasai , N. Koshika, S. Ohnuma, W.A. von, Riesemann, D.C. Bickel and M.B. Parks (1993) “Local damage to reinforced concrete structures caused by impact of aircraft engine missiles, Part 1.Test program, method and results” Nucl Eng Des 140, 387.

[2] T. Sugano , H. Tsubota , Y. Kasai , N. Koshika, C. Itoh, N. Shirai, W.A. von Riesemann, D.C. Bickel and M.B. Parks (1993) “Local damage to reinforced concrete structures caused by impact of aircraft engine missiles, Part 2.Evaluation of test results” Nucl Eng Des 140, 407–423.

[3] T. Sugano , H. Tsubota , Y. Kasai , N. Koshika, S. Orui, W.A. von Riesemann, D.C. Bickel and M.B. Parks (1993) “Full-scale aircraft impact test for evaluation of impact force” Nucl Eng Des 140, 373.

[4] Kennedy, R. P. (1976) “A review of procedures for the analysis and design of concrete structures to resist missile impact effects” Nucl Eng Des 37, 183–203.